Supplementary Information for

"Are small microplastics missing?"

Aoki and Furue

Supplementary Note 1 Derivation of total abundance

In this section, we calculate the total number and total mass of the plastic fragments. In the main text, the amplitude A is nondimensional when $S(\lambda)$ is fitted to an observed size spectrum per unit volume of sea water or it has the dimension of length cubed when the observation is a raw size spectrum as in Cózar et al. Accordingly, the following total number and mass are regarded as per unit volume of sea water or raw depending on which type of size spectrum $S(\lambda)$ denotes.

A transformation of variables $\nu' = \nu/\gamma^*$ in (4) leads to

$$S(\nu)d\nu = A\gamma^{*3}\nu'^2\frac{1}{e^{\nu'}-1}d\nu'. \tag{S1}$$

The total number of plastic fragments over $0 < \lambda < \Lambda\ (\leq L)$ can then be written as

$$N \equiv \int_{1/\Lambda}^{\infty} S(\nu)d\nu = \int_{1/\gamma^*\Lambda}^{\infty} \frac{A\gamma^{*3}\nu'^2}{e^{\nu'}-1}d\nu' \tag{S2}$$

and with this familiar formula $(e^{\nu'}-1)^{-1} = \sum_{j=1}^{\infty} e^{-j\nu'}$,

$$\begin{aligned} N &= A\gamma^{*3}\sum_{j=1}^{\infty}\int_{1/\gamma^*\Lambda}^{\infty}\nu'^2 e^{-j\nu'}d\nu' \\ &= A\gamma^{*3}\left[2\,\mathrm{Li}_3(e^{-1/\gamma^*\Lambda}) + 2\left(\frac{1}{\gamma^*\Lambda}\right)\mathrm{Li}_2(e^{-1/\gamma^*\Lambda}) - \left(\frac{1}{\gamma^*\Lambda}\right)^2\ln(1-e^{-1/\gamma^*\Lambda})\right], \end{aligned} \tag{S3a}$$

where

$$\mathrm{Li}_s(z) \equiv \sum_{j=1}^{\infty}\frac{z^j}{j^s}.$$

When $\Lambda \gg \gamma^{*-1}$,

$$N \approx A\gamma^{*3}2\,\mathrm{Li}_3(1) = \sigma A\gamma^{*3}, \tag{S3b}$$

where $\sigma \equiv 2.404$, because $\mathrm{Li}_3(1) = \sum_{j=1}^{\infty} j^{-3} \simeq 1.202$ (known as Apéry's constant; see https://oeis.org/A002117). This approximation is equivalent to $\int_{1/L}^{\infty} S(\lambda)d\lambda \approx \int_0^{\infty} S(\lambda)d\lambda$. This approximation is a natural one when $\Lambda \sim L$ because $1/\gamma^*\Lambda \sim 1/\gamma^* L = 2L\Delta h\phi/\gamma$ and this factor is therefore the ratio of the surface energy $L\Delta h\phi$ to the mean environmental energy γ. We naturally assume that $L\Delta h\phi \ll \gamma$ because otherwise not many small fragments would be generated.

Similarly, the total mass of plastics is

$$M \equiv \int_0^{\Lambda} \rho\lambda^2 \Delta h\, S(\lambda)d\lambda, \tag{S4}$$

where ρ is the mass density of the plastic material and Δh is the thickness of the original plate. After similar transformations as above,

$$M = A\gamma^*\rho\Delta h \sum_{j=1}^{\infty} \frac{e^{-j/\gamma^*\Lambda}}{j} = -A\gamma^*\rho\Delta h \ln(1 - e^{-1/\gamma^*\Lambda}) \tag{S5a}$$

$$\approx A\gamma^*\rho\Delta h \ln(\gamma^*\Lambda), \tag{S5b}$$

using the same approximation, $\gamma^*\Lambda \gg 1$, as for N. Unlike N, M depends on Λ even when $\gamma^*\Lambda \gg 1$ because the contribution of larger plastic pieces is significant to M whereas it is negligible to N.

Supplementary Note 2 Analogy with black body radiation

Our size distribution (Eqs. 4 and 5) is analogous to Planck's spectrum of black body radiation[51], which is given by[36]

$$\frac{8\pi\nu^2}{c^3}\frac{h\nu}{e^{h\nu/kT}-1}, \tag{S6}$$

where h is the Planck constant, c is the electromagnetic wave speed, k is the Boltzmann constant, and T is temperature. As compared to (4), this formula can be obtained formally if we take $A \to 2\pi h/c^3$ and $\gamma \to kT$ and multiply the right-hand side of (4) by ν. The last difference is merely due to the dimensionality of the ν-space: the numerator of our formula becomes also proportional to ν^3 if the fragmentation of plastics is three-dimensional (see below). The corresponding wavelength (size) spectrum is obtained from the relation $\lambda = c/\nu$ for Planck's and $\lambda = 1/\nu$ for our spectrum.

Planck's formula is originally derived for electromagnetic radiation within a vacuum cavity[36]. The atoms on the cavity wall absorb and emits electromagnetic waves or photons. A photon with a wavenumber of ν has an energy of $h\nu$. The term $h\nu/(e^{h\nu/kT}-1)$ in (S6) represents the expected value of the energy under an equilibrium state, and this term divided by $h\nu$ is the so called Bose distribution[37], which provides the expected value of the number of photons. Since the wavenumber interval $(\nu, \nu + d\nu)$ includes $8\pi\nu^2 d\nu/c^3$ modes per unit volume of the three-dimensional cavity, the energy spectrum is expressed in the form of the product between the number of modes and the expected value of the energy (Eq. S6).

The last point does not have a close analogy with the plastic model. As we have seen, Planck's energy distribution is essentially

$$(\text{number of modes} \propto \nu^2) \times (\text{energy of a photon } h\nu) \times (\text{Bose distribution}),$$

where the Bose distribution describes the expected number of photons for each mode. On the other hand, our plastic "wavenumber" spectrum is essentially

$$(\text{number of fragments} \propto \nu^2) \times (\text{Bose distribution}),$$

where the Bose distribution describes the expected number of original plastic pieces which are fragmented. If the original plastic piece is a block and its fragmentation is three-dimensional, the number of fragments will be proportional to ν^3 and the functional form of the plastic "wavenumber" distribution with respect to ν will be exactly the same as Planck's.

Supplementary Note 3 Superposition of size distributions

Size distribution. We explore how the size distribution is modified if multiple source regions with different parameters contribute. Here we assume that each source region contributes the same number of plastic fragments (N), which gives A in (5) as a function of γ^*:

$$A = \frac{N}{\sigma\gamma^{*3}} = \frac{N}{2.404\gamma^{*3}}$$

according to (6). In this case, the size spectrum (5) can be written as

$$S^*(\lambda; a, b^*) \equiv a\frac{b^{*3}}{\lambda^4}\frac{1}{e^{b^*/\lambda} - 1},$$

where a is a nondimensional constant and $b^* \equiv b/\gamma = 1/\gamma^*$.

We next calculate the average of $S^*(\lambda; 1, b^*)$ from $b_c^* - \Delta b^*/2$ to $b_c^* + \Delta b^*/2$. The order of magnitude of b^* is known because the value of λ that gives the peak of the size spectrum is $O(b^*)$ (it can be shown that it is approximately $0.255b^*$ from Eq. 5 and this λ value is constrained by observations. The average is calculated numerically changing b^* at an interval of 0.1 mm. For an illustration, and we look at three cases with $(b_c^*, \Delta b^*) = (4\,\text{mm}, 4\,\text{mm})$, $(7\,\text{mm}, 4\,\text{mm})$, $(5\,\text{mm}, 8\,\text{mm})$, and plot the results in Suppl. Figs. S3a, S3c, and S3e, respectively. The solid black curve plots the averaged S^*; the dashed and dotted curves plot $S^*(\lambda; 1, b_1^*)$ and $S^*(\lambda; 1, b_2^*)$, where $b_1^* \equiv b_c^* - \Delta b^*/2$ and $b_2^* \equiv b_c^* + \Delta b^*/2$.

We then fit $S^*(\lambda; a, b^*)$ to the average profile by adjusting a and b^*, which is the red curve. This is to simulate the fitting of our theoretical curve to an observation which may be a mixture of plastic pieces from different origins. Compared to the "pure" profile (red curve),

the peak of the average profile (black curve) shifts leftward, the peak value is lower, and the values are larger in the smallest size range.

The right panels of Suppl. Fig. S3 plot the error (cyan curve) of the fitting of the pure profile to the average as a function of Δb^* with the same b_c^* value as in the respective left panel, which corresponds to the maximum value of Δb^* of the right panel. As expected, the fitting error grows with Δb^*. The green curve plots the optimal b^* as a function of Δb^*. The optimal b^* changes little and stays close to b_c^* (thin gray line), indicating that the value of b^* ($= 1/\gamma^*$ by definition) obtained by fitting observations is close to its average value.

Suppl. Fig. S4 plots the average and optimal profiles from Suppl. Fig. S3a but with the horizontal axis logarithmic (panel a) and with both axes logarithmic (panel b). The difference between the two curves is qualitatively similar to the difference between the observed and the best-fit theoretical curves for Cózar et al's South Atlantic data in Fig. 3d.

Total mass. Here we explore the impacts of superposition on the total mass. Suppose that the observed size distribution is a superposition of different distributions with different values of A, γ, ϕ, L, and Δh (See Fig. 1). We denote those parameter values for each distribution by A_k, γ_k, etc. for $k = 1, \ldots, K$. Assume that the shape of the superposition is similar to a "pure" distribution as in Figs. S3a and S3c.

By fitting our model spectrum to the observed, we obtain optimal values for b^* and A. Because the size distribution is similar to the corresponding "pure" distribution, (S5a) or

(S5b) should give an accurate total mass. In the main text, we used this approach to infer the value of Δh so that the calculated total mass agrees with the observed. This approach can be formulated by, if we use the approximate form (S5b) for simplicity,

$$\frac{\rho \Delta h A}{b^*} \ln(\Lambda/b^*) = \sum_{k=1}^{K} \frac{\rho_k A_k}{c_k} \ln \frac{\Lambda}{c_k \Delta h_k},$$

where $c_k \equiv b_k^*/\Delta h_k = 2L_k^2 \phi_k/\gamma_k$. The values of A and b^* on the left-hand side are those obtained by fitting the observed distribution and Δh on the left-hand side is the inferred value. Therefore, the inferred Δh is an "average" of Δh_k's in the sense that

$$\Delta h = \frac{b^*}{\rho A \ln(b^*/\Lambda)} \sum_{k=1}^{K} \frac{\rho_k A_k}{c_k} \ln \frac{c_k \Delta h_k}{\Lambda}.$$

Obviously, the result depends on the parameters A_k, γ_k, etc. If, for example, we assume that the each source contributes an equal number of plastic fragments (N), then $A_k = b_k^{*3} N/\sigma = (c_k \Delta h_k)^3 N/\sigma$, and the resultant dependency of the inferred Δh on Δh_k is

$$\Delta h = \frac{b^*}{\rho A \ln(b^*/\Lambda)} \sum_{k=1}^{K} \frac{\rho_k c_k^2 \Delta h_k^3 N}{\sigma} \ln \frac{c_k \Delta h_k}{\Lambda}.$$

Supplementary Figures and Tables

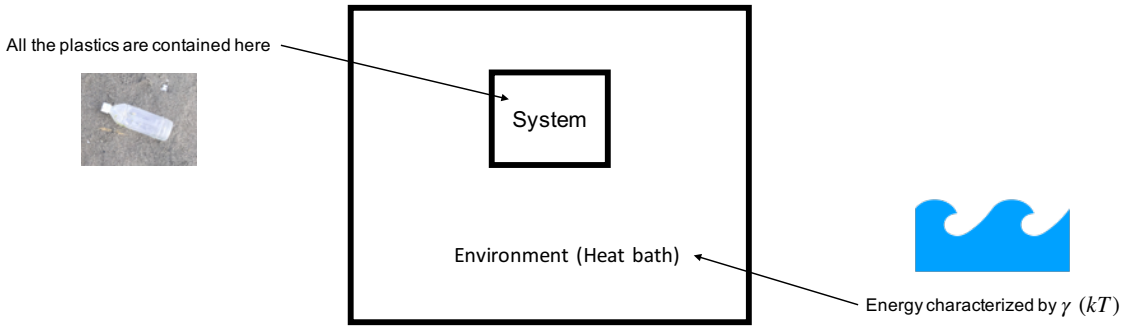

Fig. S1: Analogy between black-body radiation and microplastics. The "system" corresponds to the vacuum cavity where electromagnetic radiation occurs or the beaches where microplastics are produced. The "environment" is the heat bath, the material surrounding the cavity characterized by kT, or the energy reservoir (winds and waves) characterized by γ.

Table. S1: Optimal γ^* for different observation regions

Environmental energy γ^* [mm^{-1}]	**Region**	**Literature**
0.24	North Atlantic Ocean	Cózar et al. 2014
0.24	Around Japan	Isobe et al. 2015
0.26	Western Pacific transoceanic section	Isobe et al. 2019
0.27	South Indian Ocean	Cózar et al. 2014
0.27	South Atlantic Ocean	Cózar et al. 2014
0.35	North Pacific Ocean	Cózar et al. 2014
0.35	South Pacific Ocean	Cózar et al. 2014
0.39	Seto Inland Sea	Isobe et al. 2014

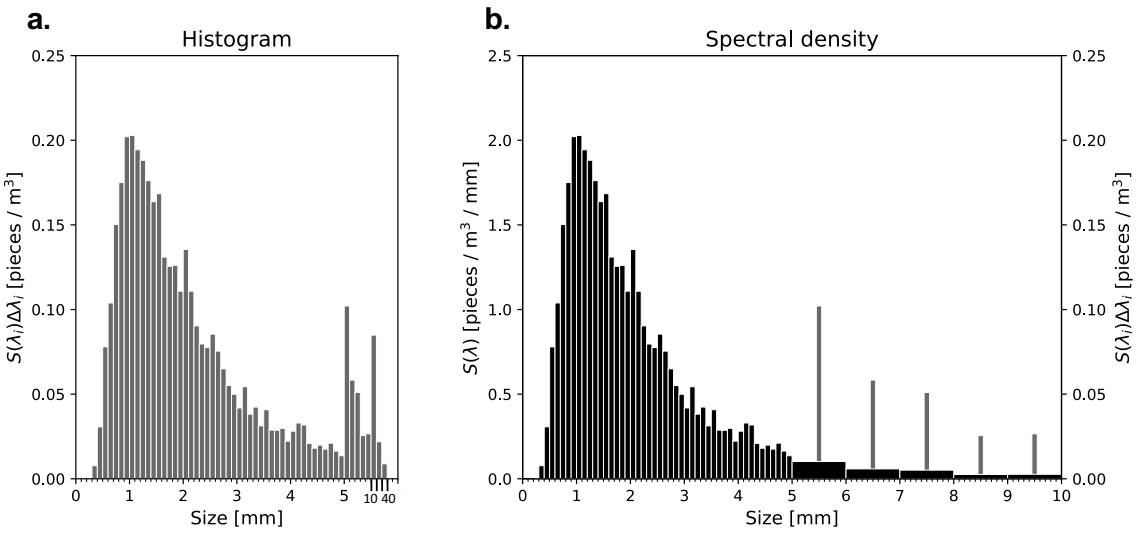

Fig. S2: Size distribution expressed as a histogram (**a**) and as a spectral density (**b**) from Isobe et al's[21] observation around Japan. The histogram is a replot of Isobe et al's Fig 2. We have obtained the data by digitizing the original figure using WebPlotDigitizer version 4.3 (https://automeris.io/WebPlotDigitizer/). The size spectral density is indicated by black bars with its scale shown on the left axis of panel (b), and the gray bars on panel (b) are the same histogram with its scale on the right axis. The spectral density is plotted in such a way that the black bars exactly coincide with the gray ones for $\lambda < 5$ mm. In panel (b), sizes larger than 10 mm are omitted because the spectral values are almost zero there.

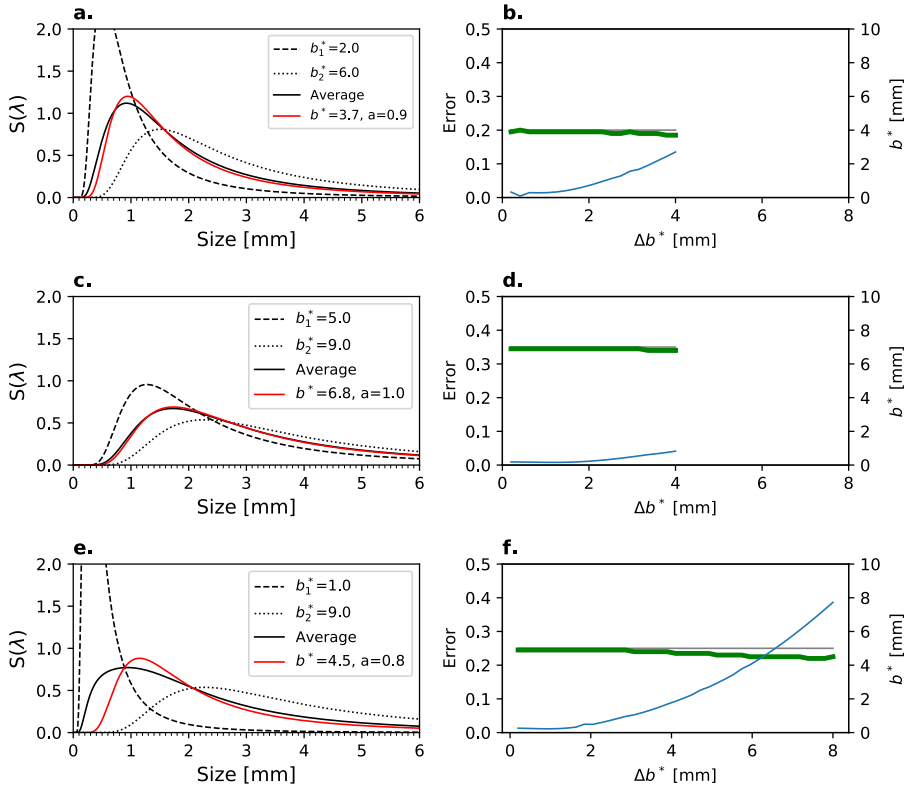

Fig. S3: Superposition of size distributions with different values of b^* ($= 1/\gamma^*$) ranging from $b_c^* - \Delta b^*/2$ to $b_c^* + \Delta b^*/2$ for **(a)** $b_c^* = 4\,\mathrm{mm}$ and $\Delta b^* = 4\,\mathrm{mm}$, **(c)** $b_c^* = 7\,\mathrm{mm}$ and $\Delta b^* = 4\,\mathrm{mm}$, and **(e)** $b_c^* = 5\,\mathrm{mm}$ and $\Delta b^* = 8\,\mathrm{mm}$. The dashed and dotted curves on the left panels are $S(\lambda; 1, b_1^*)$ and $S(\lambda; 1, b_2^*)$, respectively, where $b_{1,2}^* \equiv b_c^* \pm \Delta b^*/2$. The solid black curve is $S(\lambda; 1, b^*)$ averaged from b_1^* to b_2^*. The red curve indicates the best-fit size spectral density $S(\lambda; a_{\mathrm{opt}}, b_{\mathrm{opt}}^*)$ to the average. The right panels (**b,d,f**) show the fitting error (cyan) and the optimal b^* of the best-fit curve (green) as a function of Δb^*, where b_c^* and the maximum value of Δb^* are the same as in the corresponding left panel. The error is defined as the ratio of the norm of the difference between the average and best-fit curves to the norm of the average. The thin horizontal gray line denotes b_c^*.

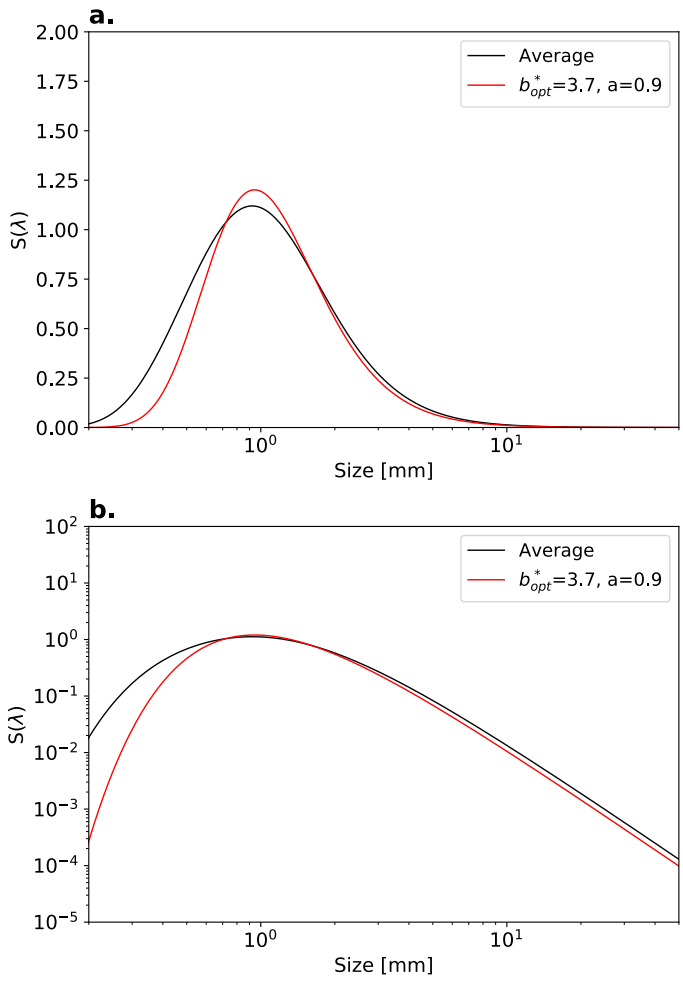

Fig. S4: Size spectral density averaged over b^* (black) and the best-fit curve (red) with optimal values for b^* and a. Both curves are the same as the black and red curves of Fig. S3a except the horizontal axis (**a**) and both axes (**b**) are logarithmic in this figure.

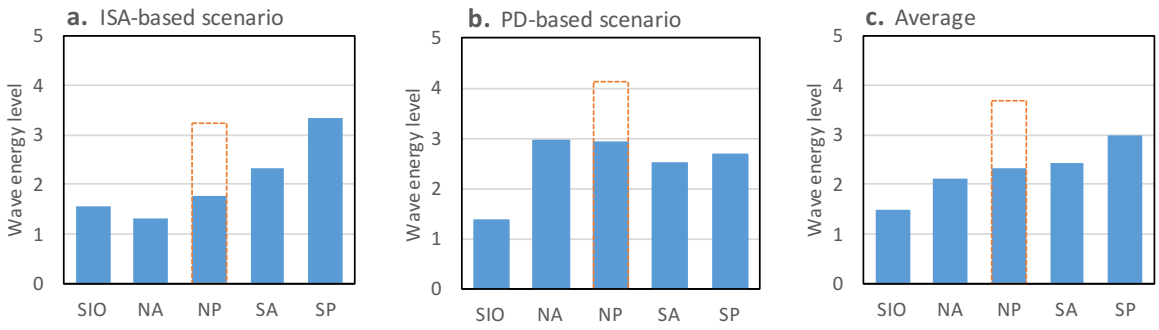

Fig. S5: Expected wave energy level for accumulation zone in Southern Indian Ocean (SIO), North Atlantic (NA), North Pacific (NP), South Atlantic (SA), and South Pacific (SP) (blue bars). Dashed orange bars denote the case without the contribution from China in the North Pacific accumulation zone.

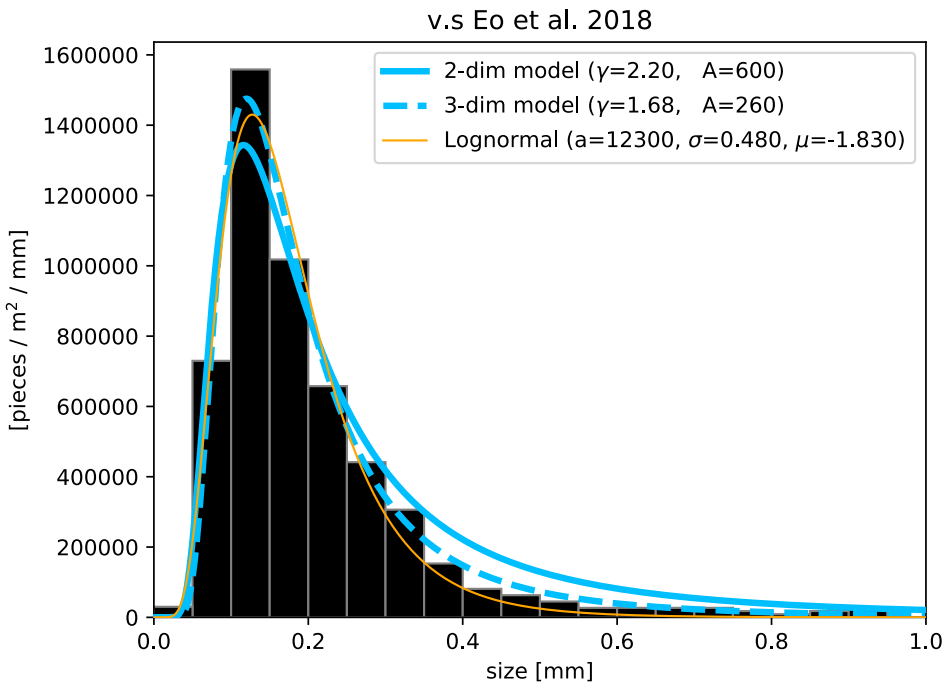

Fig. S6: Size spectral density of microplastics on Korean sand beaches collected by Eo et al[22]. See Methods for conversion from histogram into size spectrum. Blue and orange curves denote the theoretical size spectra in our model and lognormal distribution, respectively. Blue dashed curve shows theoretical size distribution multiplied by λ^{-1}. This multiplication is in consideration of a 3-dimensional process. The original plate model implicitly assumes a finite thickness sufficiently smaller than any fragment cell. However, we can consider a case that a plastic fragment with the size smaller than the plate thickness. This case may be modeled by a fracture of a cube into $n \times n \times n$ cubic cells, which can be expressed as $L^3\nu^3$, as an expansion of the original plate model. This result is one order larger than the case of the plate model, $L^2\nu^2$, with respect to ν. By the relation between the wavelength and wavenumber, this means that the size distribution in the 3-dimensional process is obtained by multiplying that in the plate model by λ^{-1}. Since Eo et al's data is the number of plastic fragments per unit area of the beach, the units of A are 10^{-9} m for 2-dimensional case (plate model) and 10^{-12} m^2 for 3-dimensional case (cube model).